J E M T
Journal of Earth and Marine Technology
homepage URL: ejurnal.itats.ac.id/jemt

Analysis of Tectonic Influence on Morphological Formation: Case Study of Gapura Pemalang Area

Huzaely Latief Sunan *[1], Maula Nurlatifah [1], FX Anjar Tri Laksono [1,2] Asmoro Widagdo[1]

[1] Department of Geological Engineering, Jenderal Soedirman University, Purbalingga, Indonesia
[2] Department of Geology and Meteorology, Faculty of Sciences, University of Pecs, Pécs, Hungary
*e-mail: huzaely.sunan@unsoed.co.id

Article info	Abstract
	Tectonic activity is closely related to the formation of landforms (morphology) in a region. The study area exhibits morphology controlled by normal fault tectonics, with blocks consisting of highlands and lowlands. This study aims to determine the extent of tectonic influence (normal faulting) on the morphology in the location. The quantitative geomorphological analysis method is used to obtain data on the level of tectonic activity present in the research area. Based on this method, it causes the formation of morphology and geological structures that affect the current surface forms. The methods used to calculate the tectonic influence are the Ratio of Valley Floor Width to Valley Height (Vf) and Mountain Front Sinuosity (Smf). Based on the results of the case study, the average Vf is 0.19, indicating class one tectonic activity and a high uplift level with V-shaped valleys. Meanwhile, the average Smf is 1.45, indicating strong tectonic activity associated with wide plains, narrow valleys, and steep hills. Based on these results, the study location falls into the category of strong tectonic activity, supported by field geological data showing right-lateral strike-slip faults and left-lateral normal faults intersecting each other.

1. Introduction

Geomorphology can help trace the processes that occur on the Earth's surface through the approach of studying the visible landforms. By understanding the geomorphological conditions of a research area, it is expected to provide information for human life and serve as a reference for development in terms of disaster management (landslides or floods), infrastructure development, and other aspects. [1] proposed that Central Java was formed by two anticlinal peaks, namely the Northern Serayu Mountains and the Southern Serayu Mountains. The Northern Serayu Mountains form a connecting line between the Bogor Zone in West Java and the Kendeng Mountains in Central Java, while the Southern Serayu Mountains are elements that emerge from the Bandung Depression Zone, which extends longitudinally in West Java.

The research area belongs to the Northern Serayu Zone. The range of the Northern Serayu Mountains is a continuation of the Bogor Zone in West Java and towards the east, it borders the Kendeng Mountains in East Java. The Northern Serayu Zone stretches from west to east with a width ranging from 30 to 50 kilometers. This zone has moderately prominent relief, forming the Slamet Mountains (3428 meters above sea level) in the western part of the zone. In its eastern end, it is covered by volcanic deposits from the Rorojembangan Mountains (2177 meters above sea level), and it slopes southwards, forming a plain known as the Serayu Depression (Serayu Basin) according to Van Bemmelen. This longitudinal depression extends from west to east through Ajibarang, Purwokerto, Banjarnegara, and Wonosobo. The Serayu Basin has a width of about 15 kilometers, which widens towards Wonosobo, but in this area, the depression is covered by the volcanic cones of Sundoro (3155 meters above sea level) and Sumbing (3371 meters above sea level).
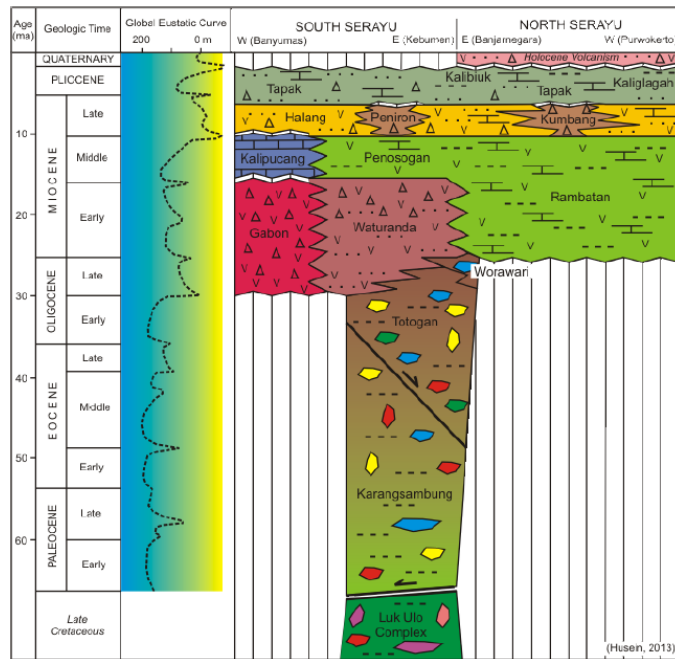
Figure 1. Regional stratigraphy of Serayu Zone [5], [6]

The level of tectonic activity in the research area can be assessed using morphotectonics through morphometric analysis. Morphometry involves the quantitative measurement of landform morphology [2]–[4]. These measurements follow the principles of geomorphology, which serve as a basis for comparing and analyzing a region's morphology and tectonic activity levels. Morphotectonics itself is influenced by the morphological conditions resulting from past tectonic activity, and tectonics themselves express the topographic features formed and can serve as indicators of ongoing tectonic movement. In the research area, the morphology is controlled by geological structures, which is why this study is necessary to determine the extent of tectonic activity in the research area and its influence on the existing morphological features.

Regional Geology

The stratigraphy of the research area consists of rocks ranging in age from Tertiary to Quaternary, arranged in a formation sequence from oldest to youngest. It includes the Pemali Formation, Rambatan Formation, Waturondo Formation, Penosogan Formation, Member of Limestone of the Halang Formation, Member of Breccia of the Halang Formation, Halang Formation, Kumbang Formation, Member of Breccia of the Tapak Formation, Member of Limestone of the Tapak Formation, Tapak Formation, Kalibiuk Formation, Kaliglagah Formation, Member of Claystone of the Ligung Formation, Ligung Formation, Mengger Formation, Gintung Formation, Linggopodo Formation, Undak Deposits, Unweathered Slamet Volcano Rocks, Lava of Mount Slamet, Lahar Deposits of Mount Slamet, Alluvial Deposits (Figure 1).

According to the Cenozoic Tectonostratigraphy of the Serayu Zone (compiled from [7]–[10], [30]-[31]), it can be concluded that the research area is composed of Tertiary intrusive rocks (Tmi(d)), the Rambatan Formation (Tmr), the Halang Formation (Tmph), and alluvial deposits (Qa).

Regional Geological Structure

The tectonic framework of Java Island is influenced by the active tectonic activity of the Eurasian Plate and the Indo-Australian Plate. As a result, three dominant geological structural patterns have developed on Java Island (Figure 2): the Meratus Pattern, which trends in the northeast-southwest direction; the Sunda Pattern, which trends in the north-south direction; and the Jawa Pattern, which trends in the west-east direction [11]–[15].
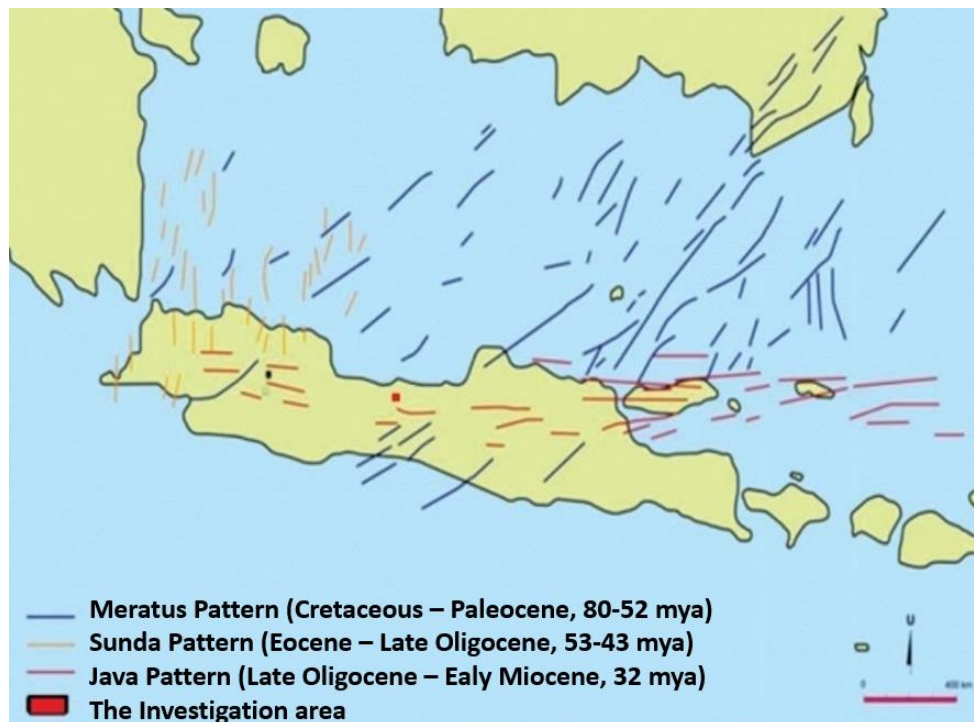
Figure 2. Geological structure pattern of Java Island [11], [16]

1. Meratus Pattern: The Meratus Pattern, which trends in the northeast-southwest direction, is the oldest pattern and formed approximately 80-53 million years ago (Late Cretaceous-Early Eocene). The Meratus Pattern formed due to tectonic compression processes, which are believed to be the initial thrusting of the Indo-Australian Oceanic Plate beneath the Sunda Shelf. This pattern is evidenced by the presence of the Cimandiri Fault.
2. Sunda Pattern: The Sunda Pattern, which trends in the north-south direction, formed approximately 53-32 million years ago (Early Eocene-Early Oligocene). The Sunda Pattern resulted from extensional tectonic activity caused by the slowing collision between the Indian and Eurasian continents, resulting in rollback during the Eocene-Early Oligocene. This pattern is characterized by north-south faults, both horizontal and thrust faults, predominantly found in the western part of Java Island.
3. Jawa Pattern: The Jawa Pattern, which trends in the west-east direction, is the youngest pattern and formed during the Neogene period. The tectonic activity associated with the Jawa Pattern reactivated the previous patterns and caused the compression of Java Island with a north-south orientation. As a result of this pattern, the Baribis Fault was formed.

According to [17], the formation and development of the North Central Java Basin are influenced by the movement and collision between the Indo-Australian Plate, moving northward, and the Eurasian Plate. The collision involves the oceanic crust of the Indo-Australian Plate and the continental crust of the Sunda Plate, resulting in the formation of an island arc system known as the Sunda Arc System. From the Middle Miocene to the present, there has been an acceleration of movement with the southward motion of the Sunda Plate, during which the North Central Java Basin developed into a Back Arc System. This acceleration has led to the activation of old faults and the formation of uplifts and depressions, with evidence of faulting still occurring today.

Based on gravity data interpretation, the structural pattern in Central Java produces three main directions [18]–[20]: a. Northwest-Southeast direction, especially in the border areas with West Java. b. Northeast-Southwest direction, found in the south and east of Central Java and around Mount Muria, representing the traces of Cretaceous-Paleocene tectonics in the form of a subduction zone. c. West-East direction, indicating the influence of Tertiary subduction in the south of Java. [21] states that the relative northward movement of the Indo-Australian Oceanic Plate with respect to the Asian continental plate during the

Cretaceous period resulted in the collision of these plates, affecting the conditions and development of the Tertiary basins formed in Indonesia, particularly on Java Island, which influenced the development of the geological structural pattern on Java Island. Based on the research on gravity data interpretation conducted by [22]–[24], the tectonic deformation of Java Island, resulting in fold patterns in the Central Java region with a west-east orientation, has been interpreted.

Regionally, the tectonic activity in Java Island has led to the development of various geological structures. The formed structural patterns reflect the dominant stress patterns from specific tectonic processes with varying orientations. The resulting stress patterns give rise to structures such as faults, fractures, and folds at various scales, ranging from regional to smaller scales. Java Island is controlled by several major structures that reflect its tectonic evolution [16], [25], [26] (Figure 2). The major structures of Java Island consist of the Meratus Structure, trending in the northeast-southwest direction; the Sumatra Structure, trending in the northwest-southeast direction; the Sunda Structure, trending in the north-south direction; and the Jawa Structure, trending in the west-east direction. The regional structures in these areas exhibit the Jawa pattern.

2. Methodology
In this research area, two methods are used, namely the calculation of the Ratio of Valley Floor width to Valley Height (Vf) and the calculation of mountain front sinuosity (Smf).

2.1 Ratio of valley Floor width to valley Height (Vf)
The calculation of the ratio of valley floor width to valley height.

$$Vf = \frac{2Vfw}{(Eld - Esc) + (Erd - Esc)}$$

Where :
Vfw   : Width at valley floor
Eld   : Elevation left side of valley (m)
Erd   : Elevation right side of valley (m)
Esc   : Elevation at valley floor (m).

Ratio of valley floor width to valley height

$$= V_f = \frac{2V_{fw}}{(E_{ld} - E_{sc}) + (E_{rd} - E_{sc})} = \frac{2000 \text{ m}}{(425 \text{ m} - 50 \text{ m}) + (500 \text{ m} - 50 \text{ m})}$$

$$= 2.4$$
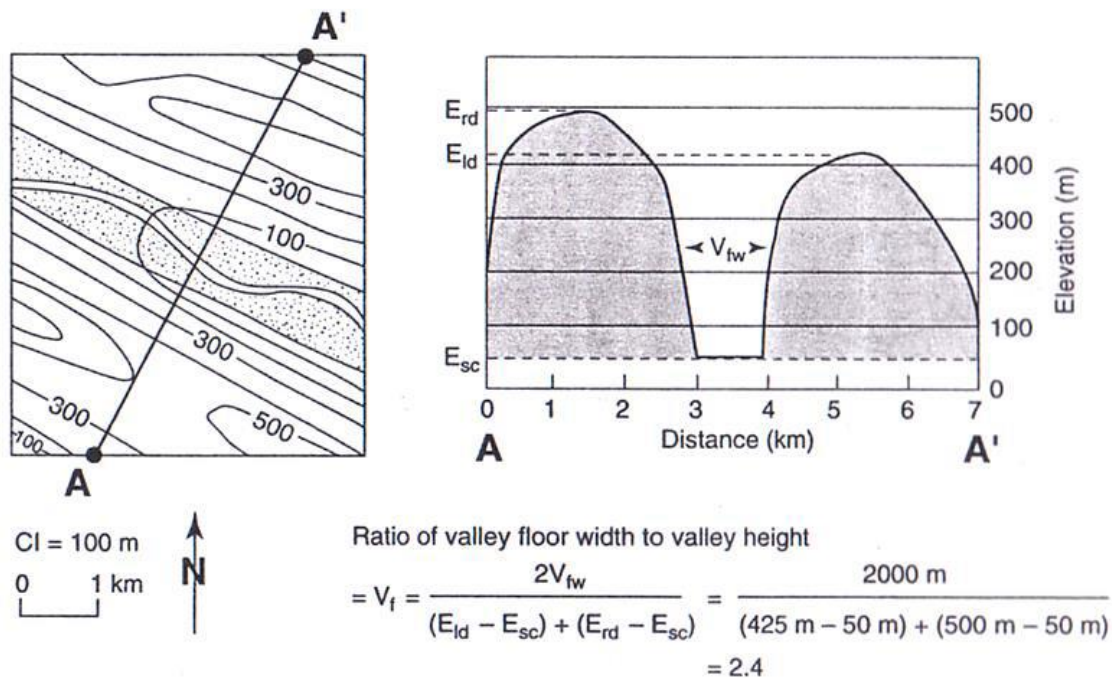
Figure 3. Calculation method of Valley Floor Width to Height Ratio

Table 1. Classification of valley floor tectonic activity and valley height [27].

Vf	Class	Explanation
< 0,50	I	High uplift level with a V-shaped valley
0,50-1,00	II	Medium uplift Level
1,00-10,00	III	Low uplift level with U-shaped valleys
>10,00	IV	Very low uplift rate with U shaped valleys

High vf values are associated with low uplift rates, resulting in wide river incision and wider valley formation. On the other hand, low vf values indicate deep valleys and reflect increased river activity due to high uplift rates (Keller and Pinter, 1996). Vf values are divided into 4 classes, as depicted in Table 4.1.

2.2 Mountain Front Sinuosity (Smf)
Mountain front sinuosity or Smf refers to the curvature of the mountain front facing the plain. Smf represents the tendency of the mountain front to follow the bends and folds of the terrain, and it is coincident with active fault zones, reflecting their active tectonic nature. A low smf value indicates active tectonics and direct uplift. As uplift decreases, the erosional processes cutting through the mountains become irregular, and the smf value increases. [27] express Smf using Equation (3) and illustrate it in Figure 3.1.

$$Smf = \frac{Lmf}{Ls} \qquad (3)$$

Where :
Lmf   : length of mountain face along the bottom (m)
Ls   : length of straight mountain face (m)
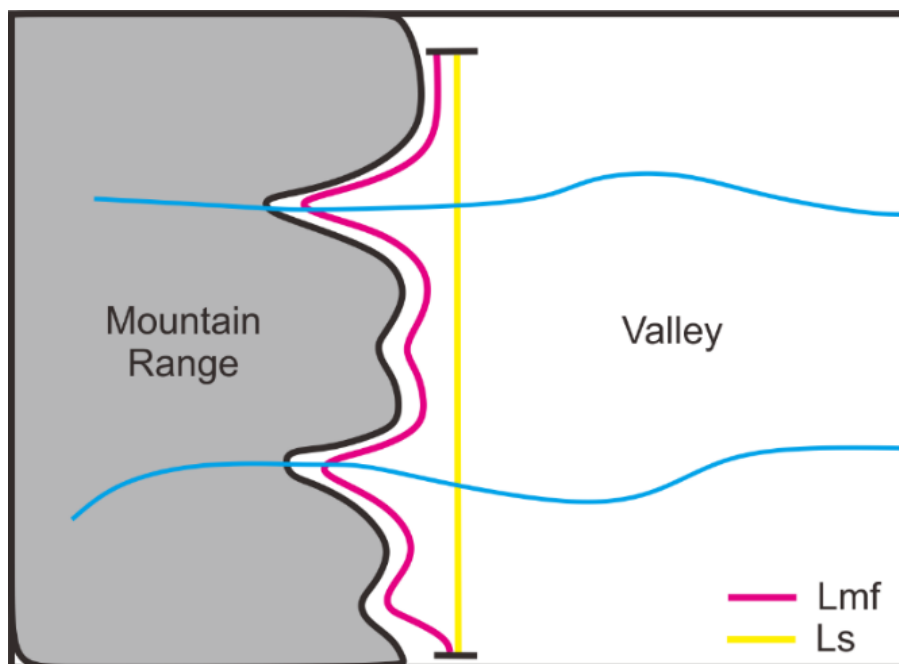
Figure 4 Calculation method of mountain face sinuosity (Smf)

Table 2. Classification of Mountain Face Sinusity (Smf) classes according to [28]

Class	Smf	Tectonic Activity	Explanation
1	1,2–1,6	Strong	Associated with wide plains, narrow valleys, and steep hills.
2	1,8–3,4	Weak	Associated with landforms of steep slopes and floodplains narrower than valley floors.
3	2,0–7,0	Non-Active	Associated with hilly landscapes.
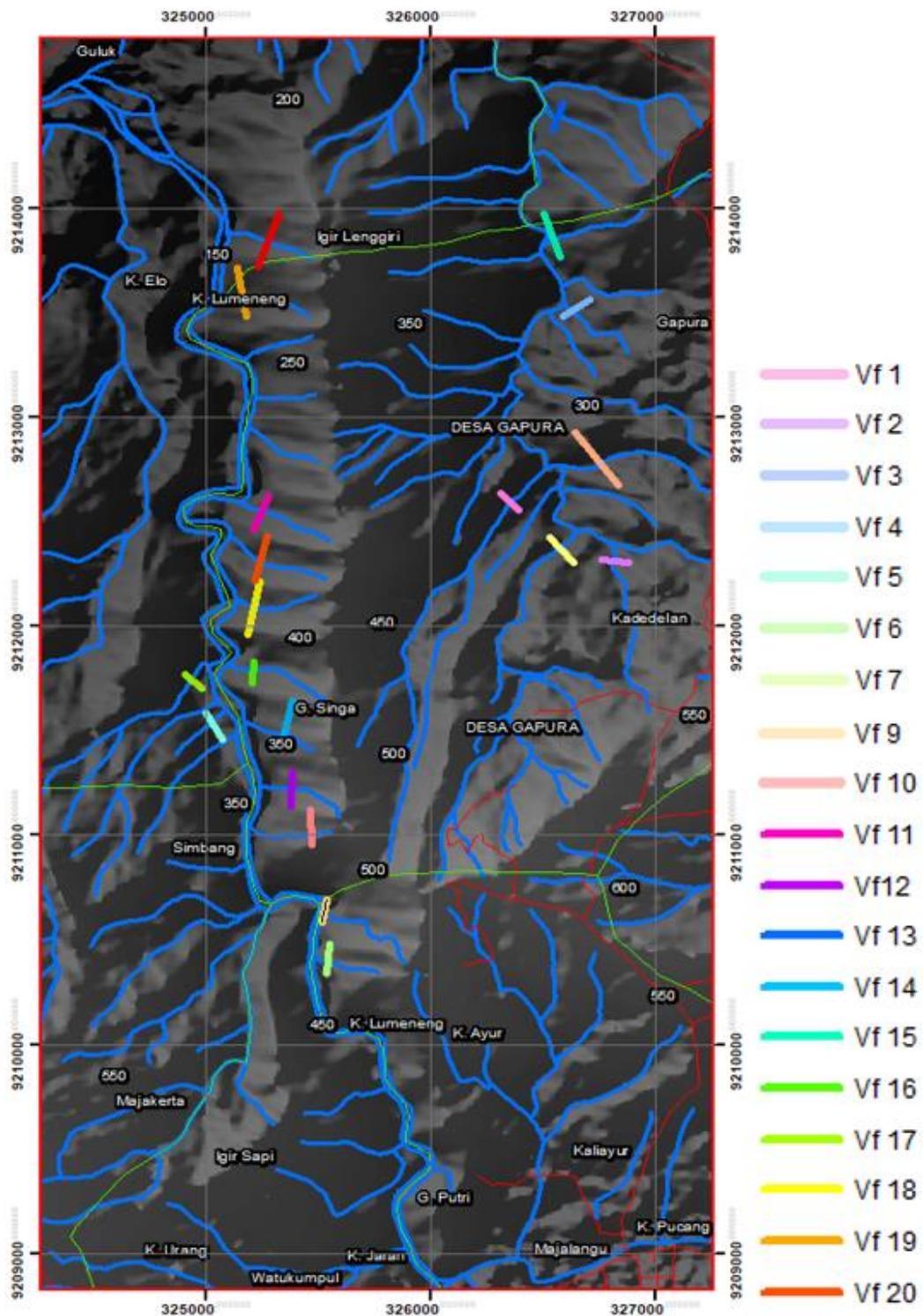
Figure 5. Withdrawal of 20 Vf data on Topographic Map

3. Results and discussions

In this study, a specific investigation was conducted to examine the tectonic activity in more detail using quantitative geomorphology methods.

3.1 Quantitative Geomorphology

Quantitative geomorphology in this research is employed to determine the presence of tectonic activity based on calculations of morphological values in the study area. Two methods were used in this research: the calculation of the Ratio of Valley Floor Width to Valley Height (Vf) and the calculation of mountain front sinuosity (Smf). In these methods, data was collected from topographic maps of the research area by drawing lines of Ratio of Valley Floor Width to Valley Height (Vf) using ARC GIS software with DEMNAS Hillshade, incorporating cross-sectional profiles that intersected two parallel hills with a valley in between (Figure 5).

The application of Arc GIS is useful for obtaining the values of Eld, Erd, Esc, and Vw, which can be observed through the cross-sectional lines of Ratio of Valley Floor Width to Valley Height (Vf) that are created. A total of 20 data points were collected from various locations within the research area (Figure 5.26). These 20 values obtained from the line drawings are then inputted into the Vf formula according to Bull and McFadden (1977). The value of 20 VF data that has been obtained, if entered into the Keller and Pinter equation has the following calculation value (see Appendix 1). From the collection of 20 data points, the average value of the Ratio of Valley Floor Width to Valley Height (Vf) is determined to be 0.19. The overall average value of Vf falls into Class 1 according to the classification of tectonic activity in valley floor and valley height by [27], indicating a high uplift rate with V-shaped valleys. A low value of Vf represents deep valleys and reflects increased activity in the rivers due to high uplift rates.

Mountain Front Sinuosity (Smf) refers to the alignment of mountains located at the front or facing the plain. Smf tends to cut along the mountain front curves with tectonic strength and corresponds to active fault zones, reflecting active tectonic activity. A low value of Smf indicates active tectonics and direct uplift. If uplift decreases, the erosion processes that cut through the mountains become irregular, and the value of Smf increases. [27] express the mountain front sinuosity (Smf) as follows:

$$Smf = Lmf / Ls \ (3)$$

Where:
Lmf   : length of mountain face along the bottom (m)
Ls   : length of straight mountain face (m)

In this method, data extraction is performed on the topographic map of the study area by drawing lines for Lmf (pink) and Ls (yellow) using the ARC GIS application. The Lmf line follows along the mountain front, while the Ls line is straight and aligned with the mountain front (Figure 6, number 1).

In the mountain front sinuosity (Smf) method, the Arc GIS application is used to obtain the values of Lmf and Ls, which can be viewed through the table in the ARC GIS application. The lengths of Lmf and Ls lines that have been drawn are determined, and 20 data points are collected from various locations within the study area (Figure 6). These 20 values obtained from the line drawing are then inputted into the Smf formula according to Keller and Pinter (1996) (see Appendix 2).

As for the value of 20 SMF data that has been obtained, if entered into the Keller and Pinter equation, it has the following calculation value. From the collection of 20 data points, the average value of Smf is found to be 1.45. The average value of mountain front sinuosity (Smf), when classified according to the Smf classification classes [29], falls into Class 1. This indicates that the study area is associated with wide plains, narrow valleys, and steep hills. A low value of mountain front sinuosity (Smf) represents active tectonics and direct uplift.

4. Conclusion

Based on the quantitative geomorphological calculations using the Vf and Smf methods, and the classification of tectonic activity [27], the study area has an average Vf value of 0.19, indicating a high uplift rate. This is reflected in the presence of deep valleys and increased river activity associated with high uplift rates. Additionally, the average Smf value is 1.45, based on the classification of mountain front sinuosity classes by [29], indicating strong tectonic activity characterized by wide plains, narrow valleys, and steep hills. Therefore, the study area, based on quantitative geomorphology, exhibits high tectonic activity.
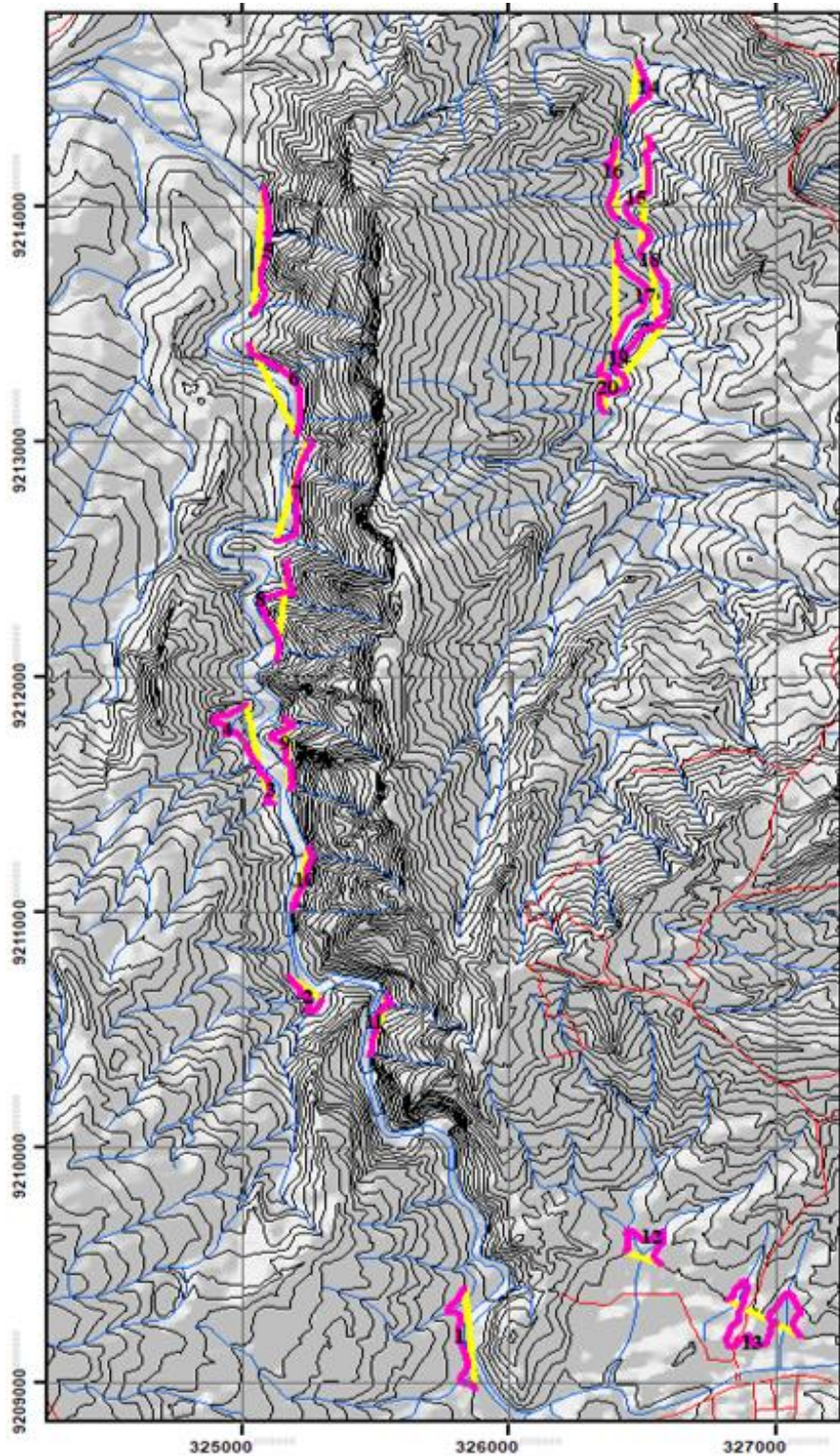
Figure 7. Drawing 20 smf data on topographic map
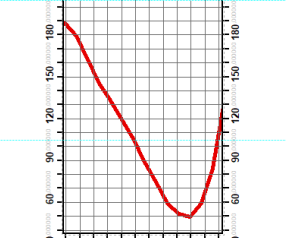
Acknowledgement
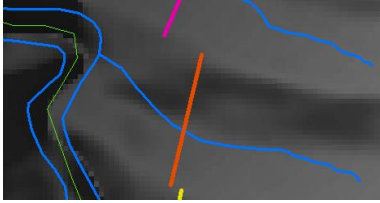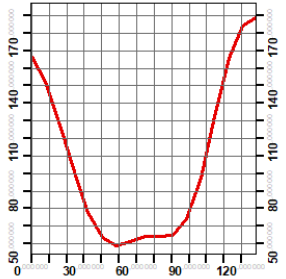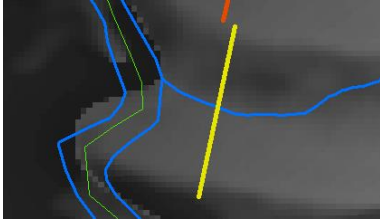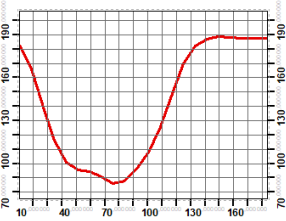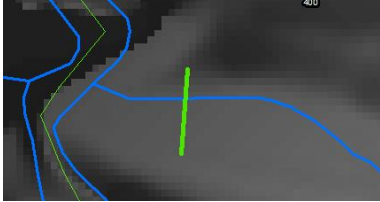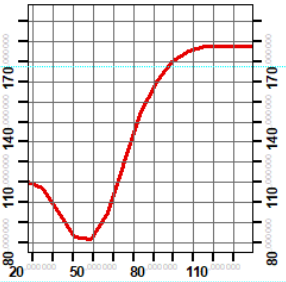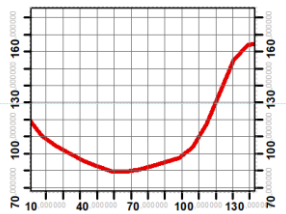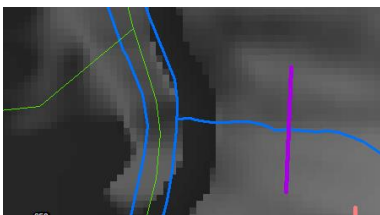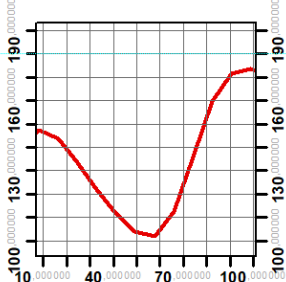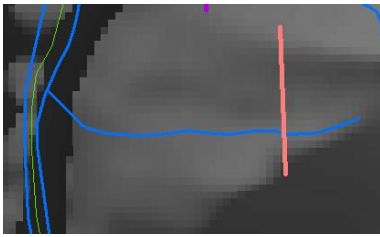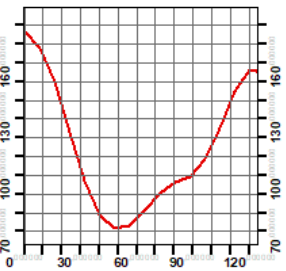
References:
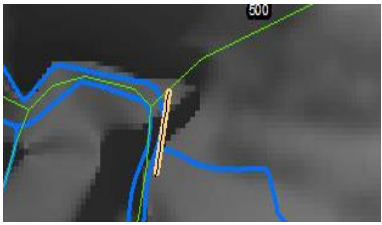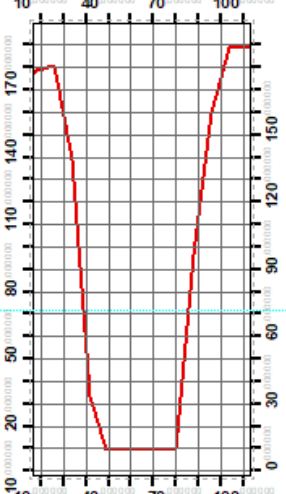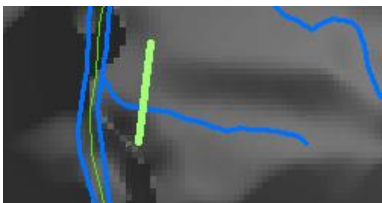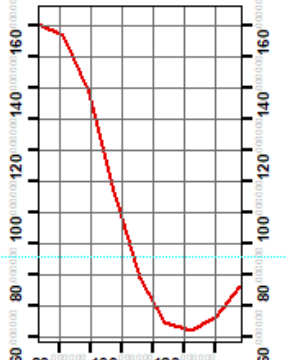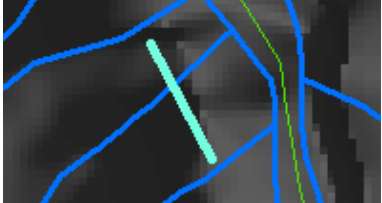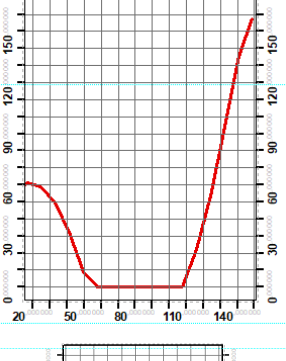
[1] E. Hidayat, D. Muslim, Z. Zakaria, H. Permana, and D. A. Wibowo, "Tectonic geomorphology of the karangsambung area, central java, indonesia," *Rud. Geol. Naft. Zb.*, vol. 36, no. 4, 2021, doi: 10.17794/rgn.2021.4.8.

[2] E. Sukiyah, E. Sunardi, N. Sulaksana, and P. P. Raditya Rendra, "Tectonic geomorphology of upper Cimanuk Drainage Basin, West Java, Indonesia," *Int. J. Adv. Sci. Eng. Inf. Technol.*, vol. 8, no. 3, 2018, doi: 10.18517/ijaseit.8.3.5441.

[3] P. Lemenkova, "Java and sumatra segments of the sunda trench: Geomorphology and geophysical settings analysed and visualized by GMT," *Bull. Serbian Geogr. Soc.*, vol. 100, no. 2, 2020, doi: 10.2298/GSGD2002001L.

[4] M. Dicky, H. Evi, M. SHIBAYAMA, and H. YAMAGUCHI, "Language Mapping Based on Geomorphology in Western Part of Java, Indonesia," 大阪教育大学紀要 第iii部門 自然科学・応用科学, vol. 58, no. 2, 2010.

[5] Aswan, Y. Zaim, Y. Rizal, and U. Prasetyo, "Molluscan evidence for slow subsidence in the bobotsari basin during the plio-pleistocene, and implications for petroleum maturity," *J. Math. Fundam. Sci.*, 2015, doi: 10.5614/j.math.fund.sci.2015.47.2.6.

[6] A. N. Saerina, I. F. Romario, and H. Nugroho, "Central Java Hydrocarbon Potential: North Serayu Petroleum System from Source to Trap Based on Geology, Geochemistry, and Geophysics Analysis," 2016. doi: 10.2523/iptc-18654-ms.

[7] A. H. Satyana and M. E. M. Purwaningsih, "Lekukan Struktur Jawa Tengah : Suatu Segmentasi Sesar Mendatar," *Yogyakarta – Cent. Java Sect. "Geology Yogyakarta Cent. Java,"* no. March, 2002.

[8] S. Zahirovic, M. Seton, and R. D. Müller, "The Cretaceous and Cenozoic tectonic evolution of Southeast Asia," *Solid Earth*, 2014, doi: 10.5194/se-5-227-2014.

[9] I. Haryanto, J. Hutabarat, A. Sudradjat, N. N. Ilmi, and D. E. Sunardi, "Tektonik Sesar Cimandiri, Provinsi Jawa Barat," *Bull. Sci. Contrib.*, 2017.

[10] Z. Zakaria, I. Ismawan, and I. Haryanto, "Identifikasi dan Mitigasi pada Zona Rawan Gempa Bumi di Jawa Barat," *Bull. Sci. Contrib. Geol.*, 2011.

[11] I. Setiadi, B. Setyanta, T. B. Nainggolan, and J. Widodo, "Delineation of Sedimentary Subbasin and Subsurface Interpretation East Java Basin in the Madura Strait and Surrounding Area Based on Gravity Data Analysis," *Bull. Mar. Geol.*, 2019, doi: 10.32693/bomg.34.1.2019.621.

[12] I. F. B. Romario, "Studi Paleogeografi Neogen Batas Cekungan Kendeng-Serayu Utara: Tantangan Dan Implikasi Pada Konsep Eksplorasi Minyak Dan Gas Bumi Di Tinggian Semarang Regional Jawa Tengah Bagian Utara," 2016.

[13] F.A.T. Laksono, S.F. Manulang, "Analisis Struktur Geologi Daerah Cinangsi Gandrungmangu Kabupaten Cilacap," *Media Bina Ilm.*, vol. 15, no. 4, pp. 4271–4278, 2020, doi: https://doi.org/10.33758/mbi.v15i4.776.

[14] F. A. T. Laksono, A. Widagdo, M. R. Aditama, M. R. Fauzan, and J. Kovács, "Tsunami Hazard Zone and Multiple Scenarios of Tsunami Evacuation Route at Jetis Beach, Cilacap Regency, Indonesia," *Sustain.*, vol. 14, no. 5, 2022, doi: 10.3390/su14052726.

[15] H. Hidayat, S. Subagio, and Z. S. Praromadani, "Interpretasi Struktur Geologi Bawah Permukaan Berdasarkan Updating Data Gaya Berat Cekungan Banyumas, Jawa Tengah," *J. Geol. dan Sumberd. Miner.*, vol. 21, no. 3, 2020, doi: 10.33332/jgsm.geologi.v21i3.524.

[16] P. H. Widjaja and D. Noeradi, "3d Properties Modeling To Support Reservoir Characteristics Of W-Itb Field In Madura Strait Area," *Bull. Mar. Geol.*, 2016, doi: 10.32693/bomg.25.2.2010.27.

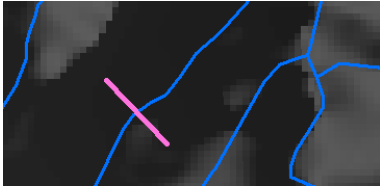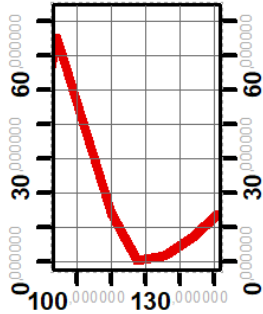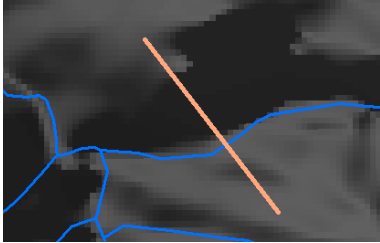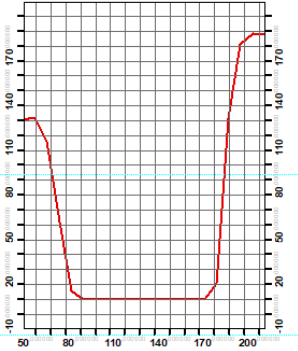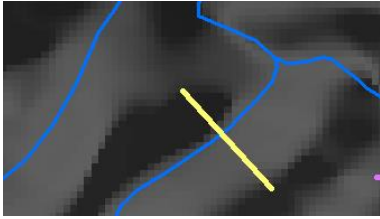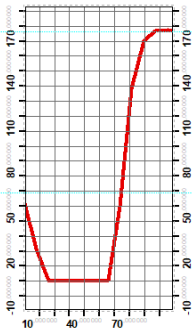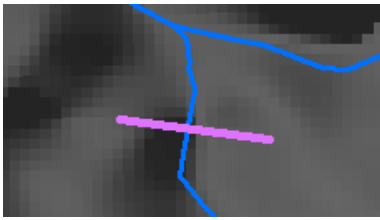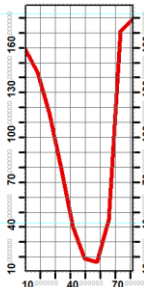[17] A. Patria and A. N. Aulia, "Structural And Earthquake Evaluations Along Java Subduction Zone,

Indonesia," *Ris. Geol. dan Pertamb.*, 2020, doi: 10.14203/risetgeotam2020.v30.1072.

[18] F. A. T. Laksono, A. Widagdo, and S. Iswahyudi, "Dynamothermal Metamorphic Sebagai Provenance Endapan Sedimen Daerah Aliran Sungai Kaligarang Semarang Berdasarkan Analisis Mineral Berat," *J. Geosaintek*, vol. 7, no. 2, 2021, doi: 10.12962/j25023659.v7i2.9097.

[19] L. Sarmili and R. A. Troa, "Keberadaan Sesar Dan Hubungannya Dengan Pembentukan Gunung Bawah Laut Di Busur Belakang Perairan Komba, Nusa Tenggara," *J. Geol. Kelaut.*, 2016, doi: 10.32693/jgk.12.1.2014.246.

[20] F. A. Kurnianto, "Proses-Proses Geomorfologi pada Bentuk Lahan Lipatan," *Maj. Pembelajaran Geogr.*, 2019.

[21] N. Horspool *et al.*, "A probabilistic tsunami hazard assessment for Indonesia," *Nat. Hazards Earth Syst. Sci.*, vol. 14, no. 11, 2014, doi: 10.5194/nhess-14-3105-2014.

[22] O. Setyandito, N. Yuwono, Nizam, F. U. Sjarifudin, Mitchell, and J. F. B. Saragih, "Hydrodynamic flow characteristics of tsunami waves impact on bearing wall layout," 2018. doi: 10.1088/1755-1315/195/1/012016.

[23] F. Widagdo, A., Pramumijoyo, S., Harijoko, A., Setijadi, R., Purwasatriya, E., Sunan, H., Aditama, M., & Tri Laksono, "Sesar Purworejo Sebagai Batas Timur Pegunungan Serayu Selatan," *Din. Rekayasa*, vol. 17, no. 1, pp. 23–32, 2021, doi: http://dx.doi.org/10.20884/1.dr.2021.17.1.335.

[24] A. H. F. Rizqi and S. Husein, "Identifikasi Batuan Sumber Hidrokarbon Formasi Rambatan di Daerah Pamulihan, Kecamatan Larangan Kabupaten Brebes, Jawa Tengah," *Pros. Semin. Nas.*, 2017.

[25] L. Rahmawan, B. Yuwono, and M. Awaluddin, "Survei Pemantauan Deformasi Muka Tanah Kawasan Pesisir Menggunakan Metode Pengukuran Gps Di Kabupaten Demak Tahun 2016 (Studi Kasus : Pesisir Kecamatan Sayung, Demak)," *J. Geod. Undip*, vol. 5, no. 4, 2016.

[26] I. W. Ambarwati, S. Feranie, and A. Tohari, "Analisis Potensi Likuifaksi Pada Wilayah Cekungan Bandung Dengan Menggunakan Metode Uji Penetrasi Konus," *Ris. Geol. dan Pertamb.*, 2020, doi: 10.14203/risetgeotam2020.v30.1038.

[27] A. Koulali *et al.*, "Crustal strain partitioning and the associated earthquake hazard in the eastern Sunda-Banda Arc," *Geophys. Res. Lett.*, 2016, doi: 10.1002/2016GL067941.

[28] A. Beniest and W. P. Schellart, "A geological map of the Scotia Sea area constrained by bathymetry, geological data, geophysical data and seismic tomography models from the deep mantle," *Earth-Science Reviews*. 2020. doi: 10.1016/j.earscirev.2020.103391.

[29] M. Bianca, C. Monaco, L. Tortorici, and L. Cernobori, "Quaternary normal faulting in southeastern Sicily (Italy): A seismic source for the 1693 large earthquake," *Geophys. J. Int.*, vol. 139, no. 2, 1999, doi: 10.1046/j.1365-246X.1999.00942.x.

[30] F. R. Widiatmoko, M. Aziz, and I. Firmansyah, "Geological Mapping of Gunungbatu and Surrounding Areas, Bodeh District, Pemalang Regency, Central Java," Journal of Earth and Marine Technology (JEMT), vol. 2, no. 1, pp. 19-29, 2021.

[31] I. Firmansyah, A. Candra, and F. R. Widiatmoko, "Geological Mapping of the Longkeyang and Surrounding Regions, Bodeh District, Pemalang Regency, Central Java," Journal of Earth and Marine Technology (JEMT), vol. 2, no. 1, pp. 9-18, 2021.

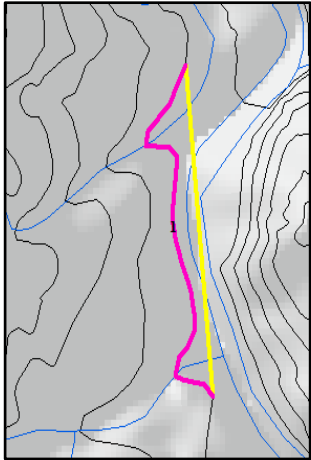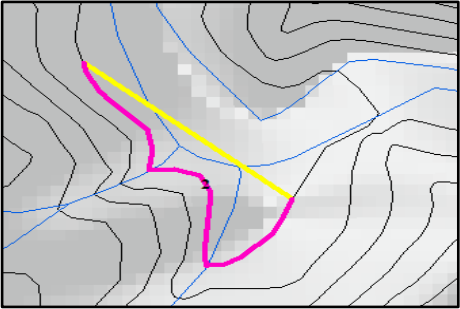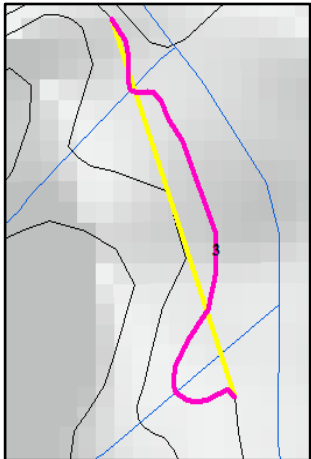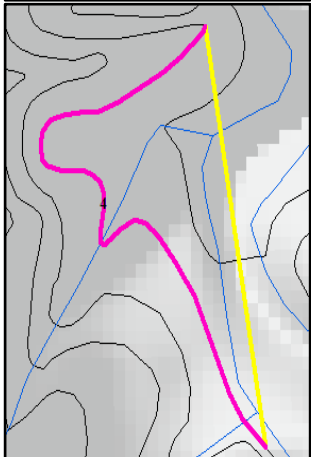**Appendix 1.** Vf value calculation data of the study area

VF	Data	Section	Vfw (m)	Eld (m)	Erd (m)	Esc (m)	Vf Value
1			20	165	190	75	0,20
2			7	112	190	40	0,06
3			10	124	133	45	0,12
4			33	169	185	10	0,20
5			9	179	190	110	0,12
6			10	168	190	107	0,14
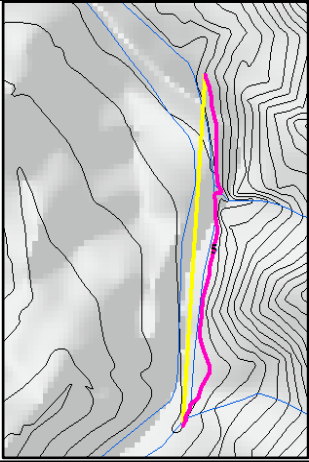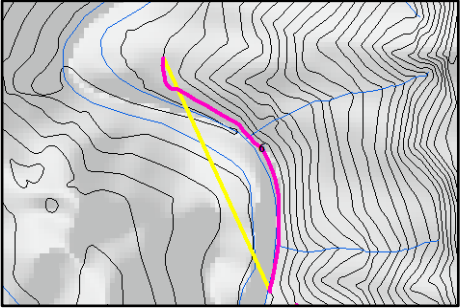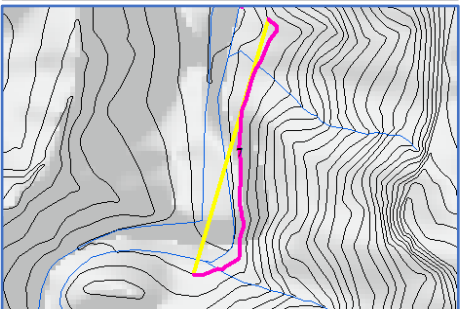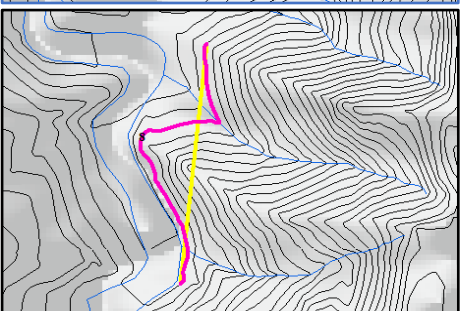
VF	Data	Section	Vfw (m)	Eld (m)	Erd (m)	Esc (m)	Vf Value
7			23	169	190	60	0,19
8			15	183	188	87	0,15
9			8	120	188	93	0,13
10			10	119	165	90	0,19
11			18	158	184	112	0,31
12			9	188	166	83	0,10
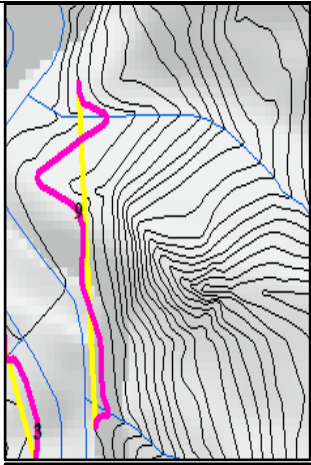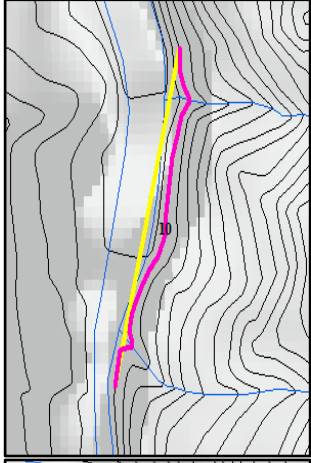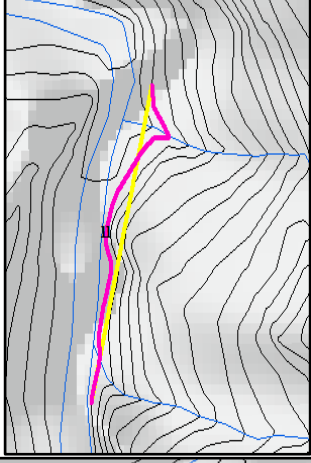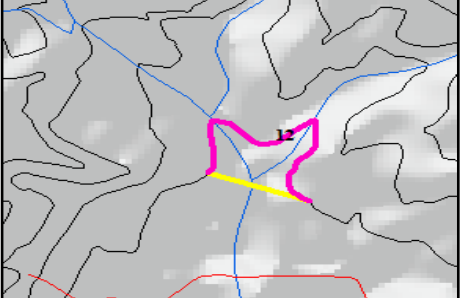
VF	Data	Section	Vfw (m)	Eld (m)	Erd (m)	Esc (m)	Vf Value
13			18	181	190	10	0,10
14			10	171	87	74	0,18
15			38	72	167	10	0,35
16			10	189	127	49	0,09
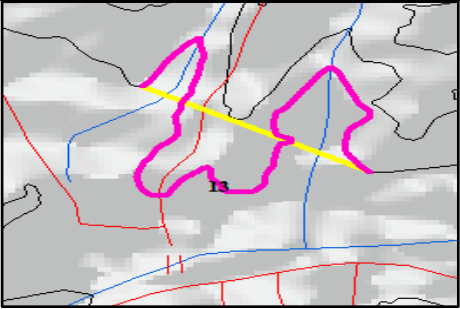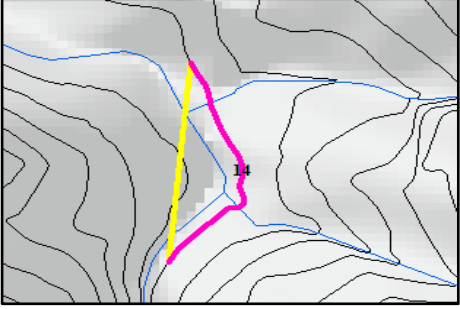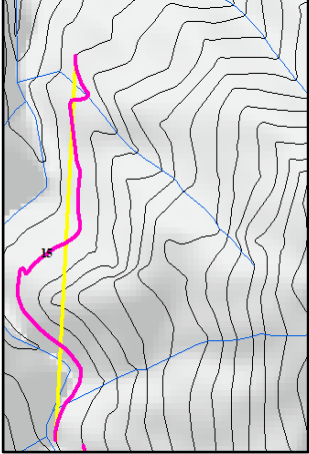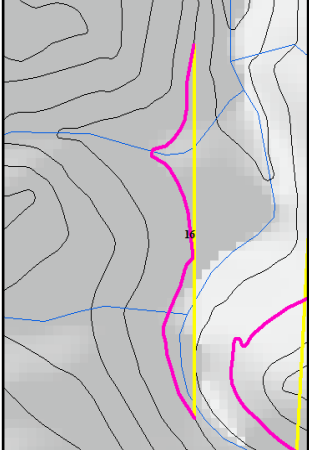
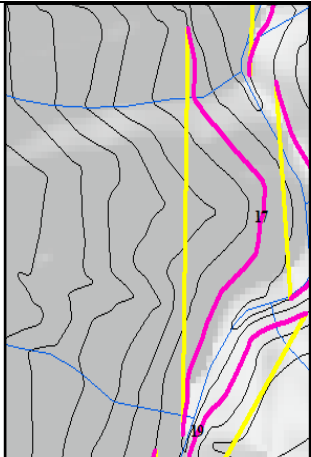| VF	Data	Section	Vfw (m)	Eld (m)	Erd (m)	Esc (m)	Vf Value
17			10	77	25	10	0,24
18			84	133	189	10	0,56
19			40	61	179	10	0,36
20			10	160	180	17	0,07
Average							0,19
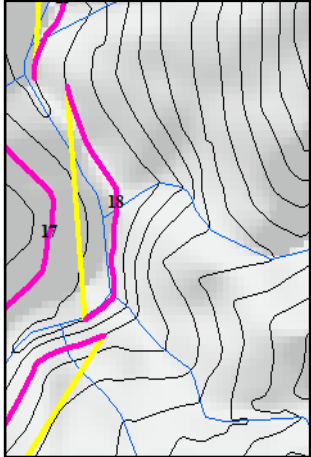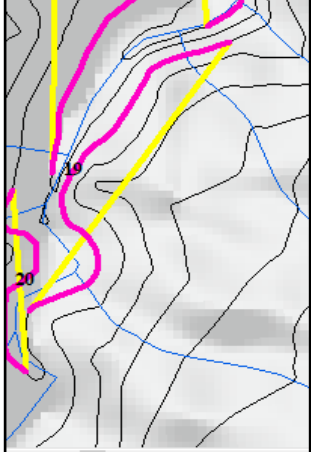
Appendix 2. Smf value calculation data of the study area
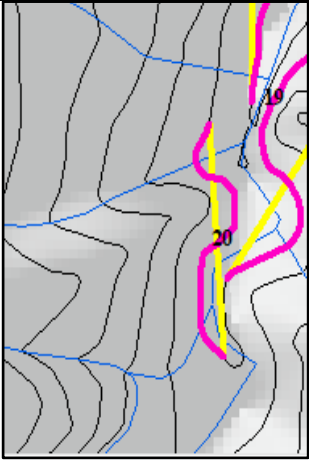
SMF	Data	Lmf (m)	Ls (M)	Smf Value
1		536,79	428,07	1,25
2		271,56	159,90	1,70
3		205,85	163,01	1,26
4		453,58	266,01	1,71

SMF	Data	Lmf (m)	Ls (M)	Smf Value
5		573,24	536,04	1,07
6		482,15	427,28	1,13
7		506,69	445,77	1,14
8		555,59	419,49	1,32

SMF	Data	Lmf (m)	Ls (M)	Smf Value
9		419,84	304,21	1,38
10		297,87	278,11	1,07
11		300,54	266,94	1,13
12		425,36	145,45	2,92

SMF	Data	Lmf (m)	Ls (M)	Smf Value
13		1105,72	318,39	3,47
14		258,46	214,84	1,20
15		646,18	511,86	1,26
16		378,00	334,09	1,13

SMF	Data	Lmf (m)	Ls (M)	Smf Value
17		580,19	494,52	1,17
18		299,13	264,82	1,13
19		448,72	369,49	1,21

SMF	Data	Lmf (m)	Ls (M)	Smf Value
20		255,44	205,13	1,25
	Average			1,45